Article

Mechanochemical Preparation of Slow Release Fertilizer Based on Glauconite–Urea Complexes

Maxim Rudmin [1,*] **, Elshan Abdullayev** [1,2] **, Alexey Ruban** [1] **, Ales Buyakov** [3,4] **and Bulat Soktoev** [1]

1   Division for Geology, Tomsk Polytechnic University, 634050 Tomsk, Russia
2   Department of Geoscience, French-Azerbaijani University (UFAZ), AZ1000 Baku, Azerbaijan
3   Institute of Strength Physics and Materials Science of Siberian Branch of Russian Academy of Sciences, 634050 Tomsk, Russia
4   Physics and Technology Faculty, Tomsk State University, 634050 Tomsk, Russia
*   Correspondence: rudminma@tpu.ru; Tel.: +78-3822-60-62-45

Abstract: We investigated the mechanochemical synthesis of complex slow release fertilizers (SRF) derived from glauconite. We studied the effectiveness of the mechanical intercalation of urea into glauconite using planetary and ring mills. The potassium-nitric complex SRFs were synthesized via a mechanochemical method mixing glauconite with urea in a 3:1 ratio. The obtained composites were analyzed using X-ray diffraction analysis, scanning electron microscopy, X-ray fluorescence analysis, and infrared spectroscopy. The results show that as duration of mechanochemical activation increases, the mineralogical, chemical, and structural characteristics of composites change. Essential modifications associated with a decrease in absorbed urea and the formation of microcrystallites were observed when the planetary milling time increased from 5 to 10 min and the ring milling from 15 to 30 min. Complete intercalation of urea into glauconite was achieved by 20 min grinding in a planetary mill or 60 min in a ring mill. Urea intercalation in glauconite occurs much faster when using a planetary mill compared to a ring mill.

Keywords: slow release fertilizer; glauconite; urea; intercalation; mechanochemical activation; milling

1. Introduction

Global agricultural production has doubled in the last 50 years, mainly due to the increased use of fertilizers and pesticides, as well as the development of new crops and technologies [1]. The global use of nitrogen fertilizers has noticeably increased from 32 million tons in 1970 to about 111.6 million tons in 2015 [2]. The use of nitrogen fertilizers is expected to grow to 130–150 million tons per year by 2050 [3]. Application of large amounts of nitrogen with low uptake efficiency can result in serious environmental pollution. The pollution can decrease the quality of water, cause the eutrophication of coastal marine ecosystems, and increase geochemical smog and global nitrous oxides, such as greenhouses gas [4–7].

The main environmental problem with excessive nitrogen fertilizer use is associated with the imbalance between nutrients and the absorption of these nutrients by plant roots, which result in the loss of chemicals and environmental pollution. Such problems can be solved using new generation fertilizers, including slow-release fertilizers (SRF) and controlled-release fertilizers (CRF) [8–12]. The main function of a SRF is to gradually deliver nutrients to plants at the required rate to reduce the excess of these components in the soil [13–15]. Urea, $(NH_2)_2CO$, is one of the most used nitrogen fertilizers due to its high proportion of nitrogen (46%) [16]. Because fertilization of agricultural soils with urea increases the risks of environmental pollution due to the distribution of excess nitrogen,

creating SRF composites that control the release of nitrogen to plants is necessary [17–19]. Based on urea as an SRF component, polymers [20,21], clay minerals such as montmorillonite [22,23], and kaolinite [24,25] were investigated. Clay minerals are environmentally stable and cheap for the synthesis of SRF [10,11,26–28].

In this study, for the first time, we investigated glauconite as an inhibitor for urea release. Glauconite is potassium phyllosilicate (clay mineral) with a dioctahedral structure [29–32] distributed in ancient marine sediments [33–38]. Due to the high content of K_2O (up to 8–9%), glauconite can serve as an independent unconventional potash fertilizer [39–45] that has a prolonged effect [46]. The aim of this research was to study the mechanochemical methods of intracalation of urea into glauconite to synthesize a polyfunctional SRF using planetary and ring mills. The SRF derived from glauconite and urea functions as a source of nitrogen and potassium.

2. Materials and Methods

2.1. Materials

Glauconite $(K_{0.65–0.69}Ca_{0–0.05}(Fe_{1.46–1.59}Mg_{0.26–0.30}Al_{0.11–0.31})_{1.96–2.06}(Si_{3.48–3.66}Al_{0.34–0.52})_4O_{10}(OH)_2$ according to scanning electron microscopy (SEM) energy dispersive X-ray spectroscopy (EDS) data [46]) was collected from the Upper Cretaceous rocks of Slavgorod and Gan'kino formations of the Bakchar deposit in Western Siberia [46]. The technology to enrich glauconite concentrate (with a proportion of glauconite up to 95%) is outlined in Rudmin et al. [44,45] as follows: wet sieving with a fraction between 80 and 500 μm and electromagnetic separation at a current of 3.5 A on an elctro-magnetic separator (EMS) 10/5 (JSC Mining Machines, Russia). The bulk chemical composition of glauconite concentrate is presented in Rudmin et al. [45] and is characterized by a K_2O content of 5.7%. urea $((NH_2)_2CO)$, composed of 46.2% nitrogen.

2.2. Mechanochemical Process

SRF was prepared by mixing glauconite (G) and urea (N) in a ratio of 3:1 (GN) and ground for various durations in a ring or planetary mill under dry conditions. Two grinding options were used to select the economically optimal method for preparing SRFs. Grinding was conducted in a ring mill (ROCKLABS Standard Ring Mill) with a rotation frequency of 700 rpm and a mass ratio of powders and grinding bodies of 1:5 for 15, 30, or 60 min to produce the composites GN-dg15, GN-dg30, and GN-dg60, respectively. Co-grinding in a planetary mill was conducted for at 5, 10, or 20 min to produce the composites GN-pm5, GN-pm10, and GN-pm20, respectively. High-energy mechanical activation of powder mixtures was performed in an AGO-2 planetary ball mill with a rotation frequency of 1820 rpm and a 1:5 mass ratio of powders to grinding bodies.

2.3. Characterization of SRFs

The characteristics of the prepared composites (6 different fertilizers) were studied using scanning electron microscopy (SEM), X-ray fluorescence analysis (XRF), Fourier transform infrared spectroscopy (FTIR), and X-ray diffraction analysis (XRD). SRFs were analyzed under TESCAN VEGA 3 SBU scanning electron microscope (Brno, Czech Republic) with an OXFORD X-Max 50 energy-dispersive adapter (High Wycombe, UK) with 20 kV accelerating voltage, specimen current of 3–12 nA, and spot diameter of approximately 2 μm. The major element concentrations of the composites were estimated using a HORIBA XGT 7200 X-ray fluorescence microscope (Kyoto, Japan) operated at a tube current of 0.5 or 1 mA, beam diameter of 1.2 mm or 10 μm, respectively, and a voltage of 50 kV with detection limit of 0.01%. The mineralogy of randomly oriented preparations of SRFs was determined using a Bruker D2 Phase X-ray diffractometer (Billerica, MA, USA) with Cu-Kα radiation at a current of 10 mA and a voltage of 30 kV. Size-fractions less than 10-μm of powdered samples were scanned from 8° to 70° 2θ, with a step size of 0.02° at a scanning rate of 1.5 s, divergence slit of 1 mm, anti-scatter slit of 3 mm, and receiving slit of 0.3 mm. IR spectra of the SRFs were obtained between 4000 and 400 cm^{-1}

using a FTIR spectrometer (Shimadzu FTIR 8400S, Kyoto, Japan) with a temperature-controlled high sensitivity detector (DLATGS) from KBr pellets with a resolution of 4 cm^{-1} to identify the chemical bond functional groups in the synthesized composites.

## 3. Results

3.1. Mineral Composition of SRFs per XRD

The results of XRD for the composite products are presented in Figure 1. Glauconite reflections are characterized by 10.1–10.9, 5.0, 4.6, 4.5, 3.8, 3.4, 3.2, 2.7, 2.5, 1.9, and 1.8 Å [47]. Urea was identified based on sharp reflections at 4.0, 3.4, and 1.8 Å. The intensity of the reflection 4.0 Å indicates the absorbed urea decreases with increasing grinding time. The first reflection shifts slightly from 10.2 to 10.9 Å (Figure 1a) and from 10.1 to 10.6 Å (Figure 1b) with increasing planetary and ring mill grinding time, respectively.
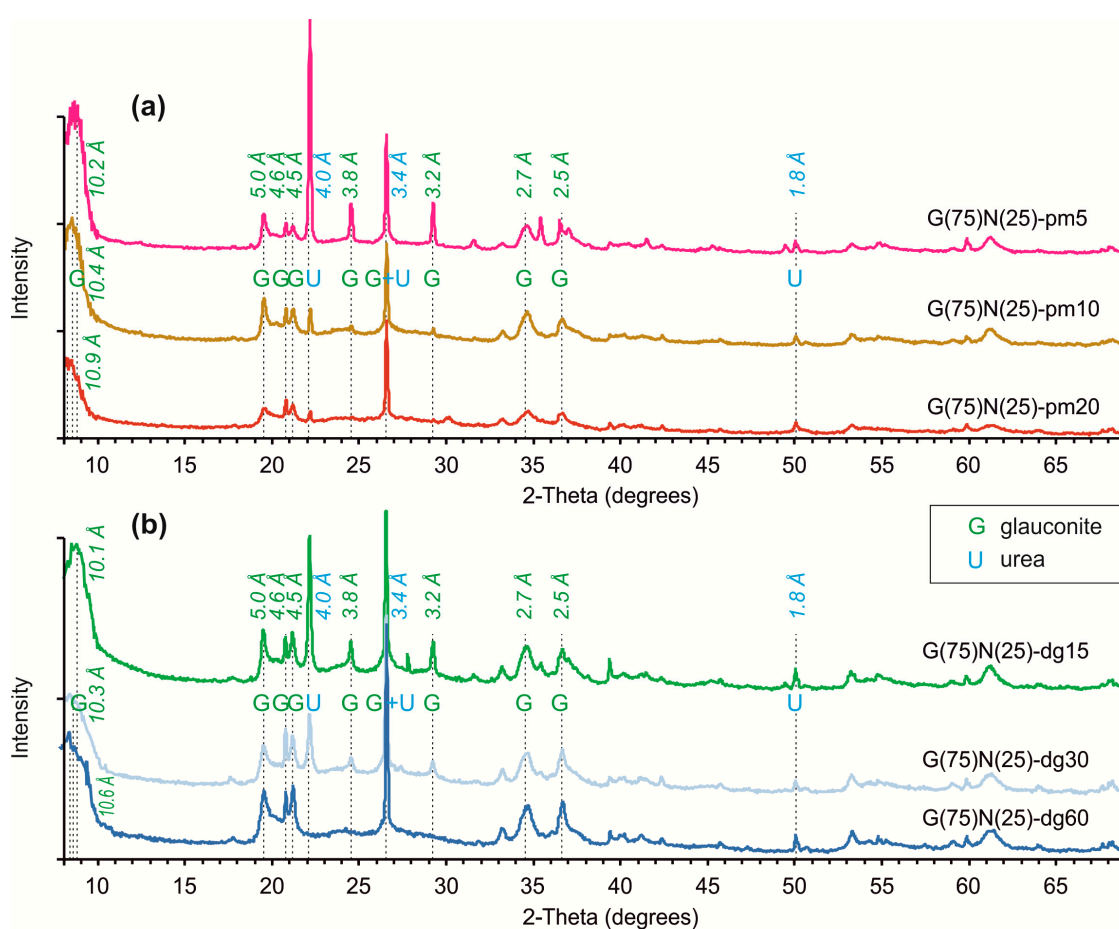
Figure 1. XRD pattern of SRF prepared by (**a**) planetary and (**b**) ring mills.

### 3.2. Morphology and Chemical Composition of SRFs per SEM-EDS and XRF

The morphology of the GN-pm5 composite is represented by relics of the glauconite structure (Figure 2a,b) with inclusions of quartz and a small amount of pyrite, as well as a surface film of urea (Figure 2c) with a thickness of some hundreds of nanometers. The length of glauconite flakes in this composite ranges from 1.4 to 2.1 μm. Composite GN-pm10 is represented by microcrystalline forms (Figure 2e) less than 1 μm, which, in some areas, are microaggregates. These microaggregates have inherited the outlines of glauconite flakes (Figure 2d). Composite GN-pm20 is characterized by a cluster of subisometric crystallites 0.4–1 μm in size (Figure 2f,g).
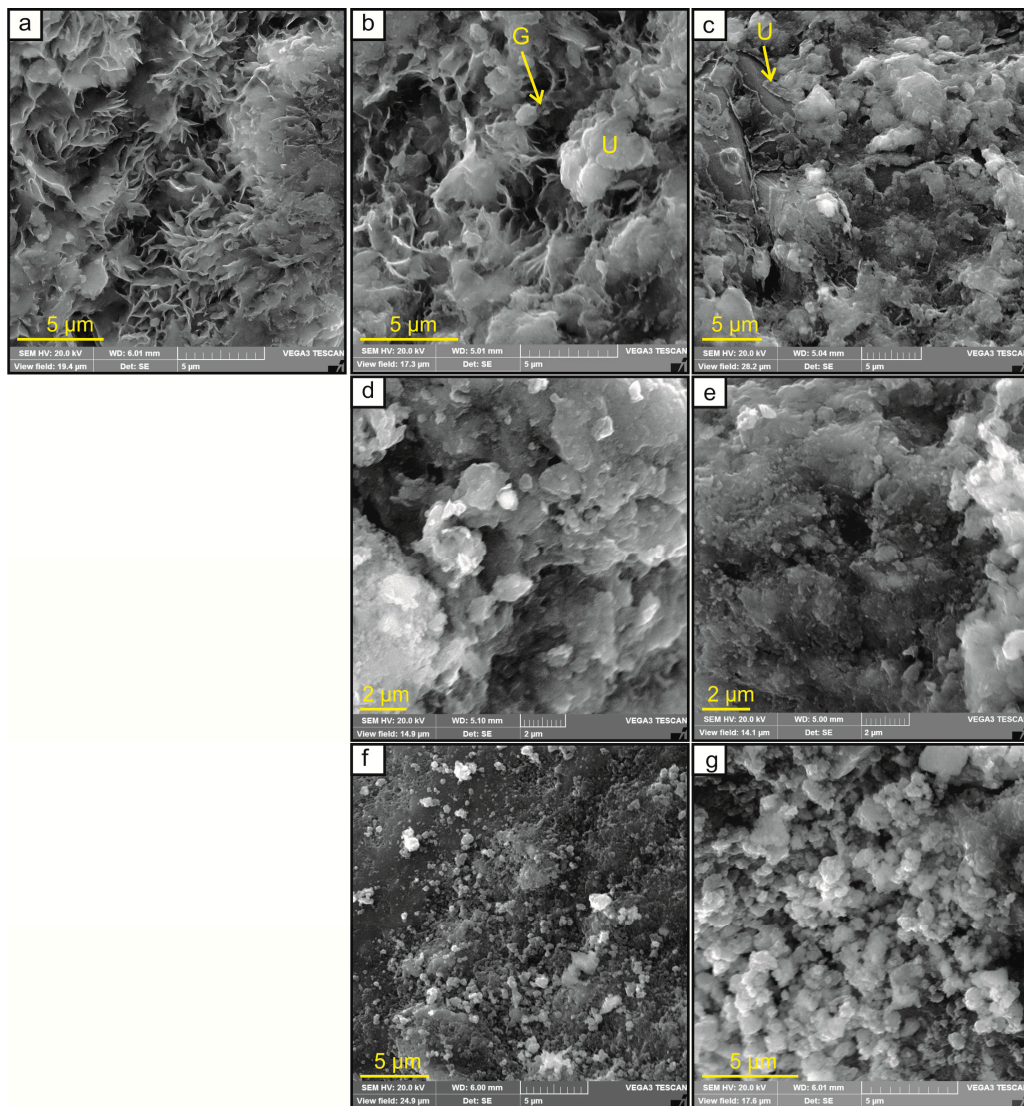
Figure 2. SEM images of SRF composites prepared by mixing glauconite (G) and urea (U) in a planetary mill: (**a**) untreated glauconite; (**b**,**c**) GN-pm5 with relics of the glauconite structure and surface film of urea; (**d**,**e**) GN-pm10 with microcrystalline forms, which cover microaggregates of glauconite flakes; (**f**,**g**) GN-pm20 with prismatic or subisometric microcrystallites.

The morphology of composites particles produced using a ring mill depends on the grinding time. The composite synthesized in 15 min (GN-dg15) is characterized by laminar, and less frequently, pseudoglobular microstructures (Figure 3a), with acicular urea microcrystallites being observed. The relics of the glauconite structure were observe in the composite (Figure 3b). After 30 and 60 min of grinding, new composites formed (GN-dg30 and GN-dg60, respectively) that consist of elongated prismatic or subisometric microcrystallites moderately ordered into domain-like clusters (Figure 3c,d).
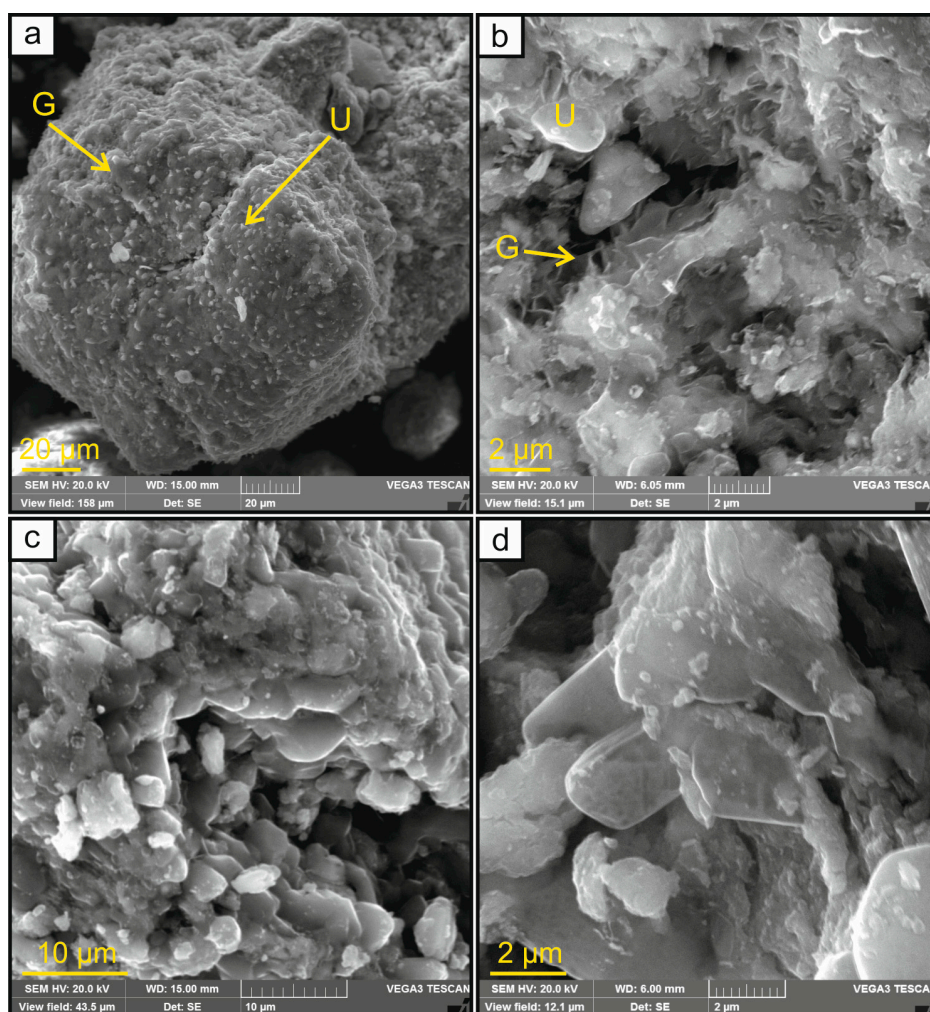
Figure 3. SEM images of SRF composites prepared by mixing glauconite (G) and urea (U) in a ring mill: (**a**,**b**) GN-dg15; (**c**) GN-dg30; (**d**) GN-dg60.

The average chemical composition of the composites is presented in Table 1. The content of the main elements in composites, obtained by grinding in planetary or ring mills, varies depending on the milling duration. The maximum amount of N_2O_5 was 17.2% in GN-dg15, and 4.2% K_2O in GN-pm10 and GN-pm20. In addition, P_2O_5 (up to 0.5%), SO_3 (up to 0.4%), CaO (up to 0.7%), and MgO (up to 3%) were present in the composites.

Table 1. Chemical composition of glauconite-urea composites.

Composites	N_2O_5	MgO	Al_2O_3	SiO_2	P_2O_5	SO_3	K_2O	CaO	TiO_2	$Fe_2O_{3(total)}$
GN-pm5	15.7	2.8	12.7	44.8	0.5	0.3	3.2	0.7	0.4	19.4
GN-pm10	11.8	2.7	8.2	43.9	0.4	0.4	4.2	0.6	0.3	27.9
GN-pm20	12.3	3.0	9.8	45.4	0.5	0.3	4.2	0.7	0.3	25.4
GN-dg15	17.2	2.7	10.1	45.3	0.3	0.2	4.1	0.6	0.2	19.8
GN-dg30	13.8	1.5	6.4	47.5	0.3	0.3	4.0	0.6	0.3	26.1
GN-dg60	16.7	2.0	7.5	44.0	0.3	0.3	3.9	0.6	0.2	25.0

3.3. Chemical Structure of SRFs Determined Using FTIR

At low frequencies, a slight elevation occurs in the characteristic peak of urea at 720 and 790 cm^{-1} in composite products (NH_2 and CO vibrations), with the maximum occurring for 20- and 60-min intercalation in the planetary (Figure 4a) and ring (Figure 4b) mills. Characteristic peaks of

glauconite [48] in the composites are as follows (cm^{-1}): 435 (Si–O band), 460 (Si–O–Si band), 490 (Si–O–Fe bend), 1025 (Si–O stretch). The asymmetric peak (NH$_2$ strain) at 1155 cm^{-1} decreases with increasing grinding time. CN asymmetric deformations at 1465 cm^{-1} are characteristic of all composites. The characteristic vibrations at 1610, 1620, and 1670 cm^{-1} are associated with the variations in urea CO stretching, and NH$_2$ and NH deformations, respectively. The peaks at 3345 and 3450 cm^{-1} correspond to the stretching of NH and NH$_2$, respectively. Peaks around 2950–2900 cm^{-1} for composites produced by the ring mill (Figure 4b) are probably organic admixtures of glauconite [47] that were decomposed by planetary grinding.
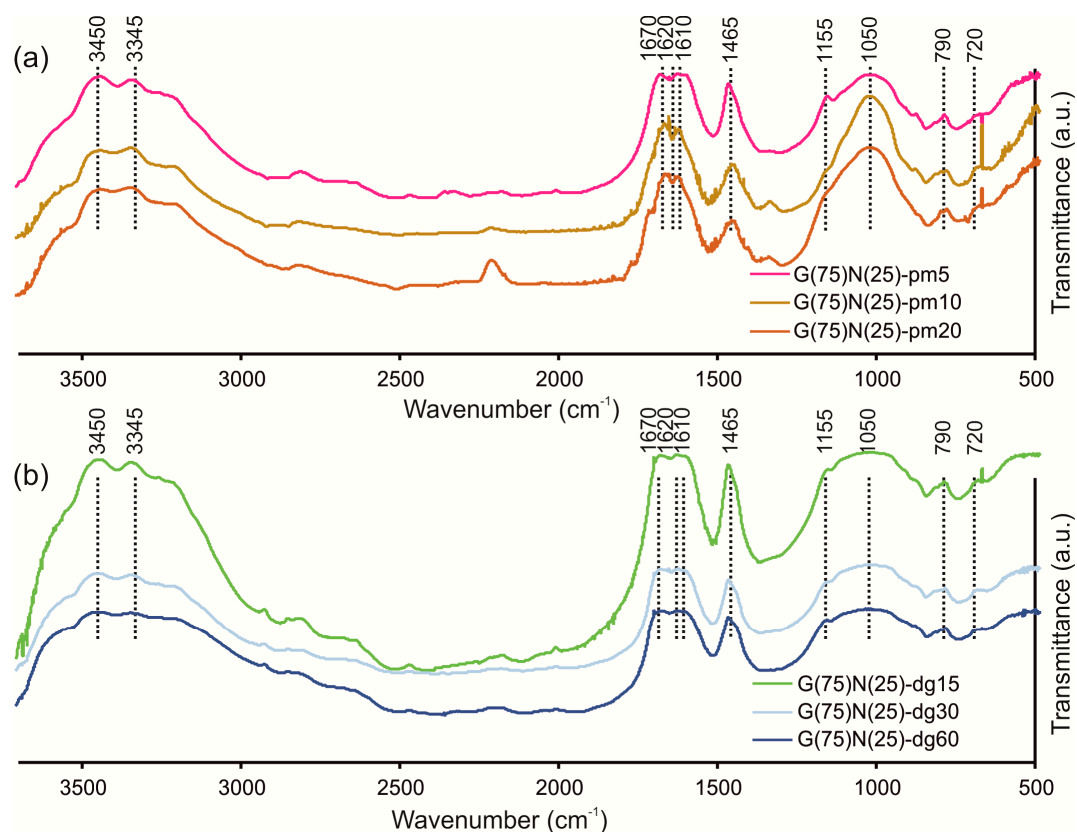
Figure 4. FTIR spectra of composite prepared by (**a**) planetary and (**b**) ring milling.

4. Discussion

Changes in the mineralogical composition of the SRF composites were investigated using XRD. As the grinding time in a ring or planetary mill increases, the intensity of the peak decreases at 4.0 Å (Figure 1), which indicates a decrease in the absorbed urea. The shifts in the first reflection (between 10.1 and 10.9 Å) during grinding indicate the increasing degree of urea intercalation into glauconite. Absorbed urea disappears when ground in a ring mill for 60 min (Figure 1a) and in a planetary mill for 20 min (Figure 1b). The morphology of the composites changes with increasing mill grinding duration. For the products synthesized using a planetary mill, with increasing grinding time from 5 to 10 min, the scaly structure of the clay mineral and the surface film of urea disappear and homogeneous microcrystallites appear. During this grinding time (between 5 and 10 min for a planetary mill), amorphization of urea likely occurred with the subsequent formation of microcrystallites, which affected the sharp decrease in the XRD peak (4.0 Å) of absorbed urea (Figure 1a). Twenty minutes of grinding in a planetary mill and 60 min in a ring mill produced composites with a homogeneous microcrystalline mass with contents of 12.3% and 16.7% N$_2$O$_5$ and 4.2% and 3.9% K$_2$O, respectively, as well as impurities in the form of complex nutrients, namely P, S, Fe, Ca, and Mg. The presence of pyrite in composites synthesized quickly (5 min in a planetary mill or 15 min in a ring mill) indicates

the integrity of the initial mineral structure of glauconite, which is characterized by the presence of sulfides [38].

The main chemical composition of the composites (Table 1) depends on the composition of the initial glauconite, which has already been shown to have a positive influence as a mineral fertilizer [44,46]. The produced glauconite–urea complex fertilizers can serve as a source of exchangeable P, Ca, and Mg [46]. Preservation of the chemical composition and microcrystalline form of nitrogen according to SEM prevent the decomposition of urea or its complete amorphization during mechanochemical activation with glauconite.

IR spectroscopy of the synthesized composites demonstrated the interaction of urea molecules with glauconite molecules (Figure 4). Increasing the grinding time in planetary or ring mills decreased the intensity of asymmetric peaks of C–N vibrations at 720, 790, and 1155 cm^{-1}. The intensity of the symmetric deformation of N–H at 1465 cm^{-1} decreased as well, but peaks of the clay minerals remained. The change in the intensity of the C–N and N–H strains can be explained by the intercalation of these molecules into the interlayer space [21,23,49,50] of the dioctahedral mineral (glauconite). This is consistent with the relatively stable chemical composition of the composites (Table 1) and XRD spectra (Figure 1). Small changes in the chemical composition of composites depend on the temperature increase during mechanochemical activation, and as a result, local decomposition of urea [51].

Full intercalation of maturing of glauconite and urea (in a 3:1 ratio) is achieved with a 20 min synthesis in a planetary mill or 60 min in a ring mill. These results are consistent with the data on the mechanochemical activation of montmorillonite [23] and kaolinite [25] when using them as SRF. Compounds based on glauconite and urea, produced using mechanochemical methods, are recommended for testing as potassium–nitrogen complex mineral SRFs.

5. Conclusions

With increasing mechanical activation time, we observed mineralogical, chemical, and structural changes in the composites. Substantial modifications associated with a decrease in the absorbed urea and formation of microcrystallites were observed with increasing planetary milling time from 5 to 10 min and increasing ring milling time from 15 to 30 min. The decrease in the intensities of NH$_2$, NH, CN, and CO deformations on the IR spectra of composites confirms the intercalation of these molecules into the interlayer of glauconite.

The potassium-nitric complex SRFs were synthesized via the mechanochemical method of mixing glauconite with urea in a 3:1 ratio. Complete intercalation of urea into glauconite was achieved by 20 min abrasion in a planetary mill or 60 min abrasion in a ring mill.

Author Contributions: M.R. conceived and designed the study. M.R., A.R., A.B., and B.S. performed the laboratory investigations. M.R., E.A., and A.B. analyzed the data. M.R., E.A., and A.R. contributed materials. M.R. and E.A. wrote the paper.

References

1. Tilman, D.; Cassman, K.G.; Matson, P.A.; Naylor, R.; Polasky, S. Agricultural sustainability and intensive production practices. *Nature* **2002**, *418*, 671–677. [CrossRef] [PubMed]
2. FAO. *Current World Fertilizer Trends and Outlook to 2015*; FAO: Rome, Italy, 2015.
3. Matson, P.A.; Parton, W.J.; Power, A.G.; Swift, M.J. Agricultural intensification and ecosystem properties. *Science* **1997**, *277*, 504–509. [CrossRef] [PubMed]

4. Ju, X.T.; Xing, G.X.; Chen, X.P.; Zhang, S.L.; Zhang, L.J.; Liu, X.J.; Cui, Z.L.; Yin, B.; Christie, P.; Zhu, Z.L.; et al. Reducing environmental risk by improving N management in intensive Chinese agricultural systems. *Proc. Natl. Acad. Sci. United States Am.* **2009**, *106*, 3041–3046. [CrossRef] [PubMed]

5. Zhang, Z.S.; Chen, J.; Liu, T.Q.; Cao, C.G.; Li, C.F. Effects of nitrogen fertilizer sources and tillage practices on greenhouse gas emissions in paddy fields of central China. *Atmos. Environ.* **2016**, *144*, 274–281. [CrossRef]

6. Akiyama, H.; Yan, X.; Yagi, K. Evaluation of effectiveness of enhanced-efficiency fertilizers as mitigation options for N_2O and NO emissions from agricultural soils: Meta-analysis. *Glob. Chang. Biol.* **2010**, *16*, 1837–1846. [CrossRef]

7. Vitousek, P.M.; Naylor, R.; Crews, T.; David, M.B.; Drinkwater, L.E.; Holland, E.; Johnes, P.J.; Katzenberger, J.; Martinelli, L.A.; Matson, P.A.; et al. Nutrient imbalances in agricultural development. *Science* **2009**, *324*, 1519–1520. [CrossRef] [PubMed]

8. Sharma, G.C. Controlled-release fertilizers and horticultural applications. *Sci. Hortic.* **1979**, *11*, 107–129. [CrossRef]

9. Oertli, J.J. Controlled-release fertilizers. *Fertil. Res.* **1980**, *1*, 103–123. [CrossRef]

10. Ni, B.; Liu, M.; Lu, S.; Xie, L.; Wang, Y. Environmentally Friendly Slow-Release Nitrogen Fertilizer. *J. Agric. Food Chem.* **2011**, *59*, 10169–10175. [CrossRef]

11. Borges, R.; Brunatto, S.F.; Leitão, A.A.; De Carvalho, G.S.G.; Wypych, F. Solid-state mechanochemical activation of clay minerals and soluble phosphate mixtures to obtain slow-release fertilizers. *Clay Miner.* **2015**, *50*, 153–162. [CrossRef]

12. Trenkel, M.E. *Controlled-Release and Stabilized Fertilizers in Agriculture*; International Fertilizer Industry Association: Paris, France, 1997.

13. Teodorescu, M.; Lungu, A.; Stanescu, P.O.; Neamţu, C. Preparation and properties of novel slow-release NPK agrochemical formulations based on poly (acrylic acid) hydrogels and liquid fertilizers. *Ind. Eng. Chem. Res.* **2009**, *48*, 6527–6534. [CrossRef]

14. Liang, R.; Liu, M.; Wu, L. Controlled release NPK compound fertilizer with the function of water retention. *React. Funct. Polym.* **2007**, *67*, 769–779. [CrossRef]

15. Liang, R.; Liu, M. Preparation and properties of coated nitrogen fertilizer with slow release and water retention. *Ind. Eng. Chem. Res.* **2006**, *45*, 8610–8616. [CrossRef]

16. Ni, B.; Liu, M.; Lü, S. Multifunctional slow-release urea fertilizer from ethylcellulose and superabsorbent coated formulations. *Chem. Eng. J.* **2009**, *155*, 892–898. [CrossRef]

17. González, M.E.; Cea, M.; Medina, J.; González, A.; Diez, M.C.; Cartes, P.; Monreal, C.; Navia, R. Evaluation of biodegradable polymers as encapsulating agents for the development of a urea controlled-release fertilizer using biochar as support material. *Sci. Total. Environ.* **2015**, *505*, 446–453. [CrossRef]

18. Yamamoto, C.F.; Pereira, E.I.; Mattoso, L.H.C.; Matsunaka, T.; Ribeiro, C. Slow release fertilizers based on urea/urea–formaldehyde polymer nanocomposites. *Chem. Eng. J.* **2016**, *287*, 390–397. [CrossRef]

19. Liu, J.; Yang, Y.; Gao, B.; Li, Y.C.; Xie, J. Bio-based elastic polyurethane for controlled-release urea fertilizer: Fabrication, properties, swelling and nitrogen release characteristics. *J. Clean. Prod.* **2019**, *209*, 528–537. [CrossRef]

20. Pang, W.; Hou, D.; Wang, H.; Sai, S.; Wang, B.; Ke, J.; Wu, G.; Li, Q.; Holtzapple, M.T. Preparation of microcapsules of slow-release NPK compound fertilizer and the release characteristics. *J. Braz. Chem. Soc.* **2018**, *29*, 2397–2404. [CrossRef]

21. Baldanza, V.A.R.; Souza, F.G.; Filho, S.T.; Franco, H.A.; Oliveira, G.E.; Caetano, R.M.J.; Hernandez, J.A.R.; Ferreira Leite, S.G.; Furtado Sousa, A.M.; Nazareth Silva, A.L. Controlled-release fertilizer based on poly(butylene succinate)/urea/clay and its effect on lettuce growth. *J. Appl. Polym. Sci.* **2018**, *47*, 46858. [CrossRef]

22. Hermida, L.; Agustian, J. Slow release urea fertilizer synthesized through recrystallization of urea incorporating natural bentonite using various binders. *Environ. Technol. Innov.* **2019**, *13*, 113–121. [CrossRef]

23. Golbashy, M.; Sabahi, H.; Allahdadi, I.; Nazokdast, H.; Hosseini, M. Synthesis of highly intercalated urea-clay nanocomposite via domestic montmorillonite as eco-friendly slow-release fertilizer. *Arch. Agron. Soil Sci.* **2017**, *63*, 84–95. [CrossRef]

24. Rutkai, G.; Makó, É.; Kristóf, T. Simulation and experimental study of intercalation of urea in kaolinite. *J. Colloid Interface Sci.* **2009**, *334*, 65–69. [CrossRef]

25.　Makó, É.; Kristóf, J.; Horváth, E.; Vágvölgyi, V. Kaolinite–urea complexes obtained by mechanochemical and aqueous suspension techniques—A comparative study. *J. Colloid Interface Sci.* **2009**, *330*, 367–373. [CrossRef] [PubMed]

26.　Borges, R.; Baika, L.M.; Grassi, M.T.; Wypych, F. Mechanochemical conversion of chrysotile/K_2HPO_4 mixtures into potential sustainable and environmentally friendly slow-release fertilizers. *J. Environ. Manag.* **2018**, *206*, 962–970. [CrossRef] [PubMed]

27.　Fatimah, I.; Yudha, S.P.; Rubiyanto, D.; Widodo, I.D. Methenamine-smectite clay as slow release fertiliser: Physicochemical and kinetics study. *Chem. Eng. Trans.* **2017**, *56*, 1639–1644.

28.　Borges, R.; Prevot, V.; Forano, C.; Wypych, F. Design and kinetic study of sustainable potential slow-release fertilizer obtained by mechanochemical activation of clay minerals and potassium monohydrogen phosphate. *Ind. Eng. Chem. Res.* **2017**, *56*, 708–716. [CrossRef]

29.　Drits, V.A. Isomorphous cation distribution in celadonites, glauconites and Fe-illites determined by infrared, Mössbauer and EXAFS spectroscopies. *Clay Miner.* **1997**, *32*, 153–179. [CrossRef]

30.　Meunier, A.; El Albani, A. The glauconite-Fe-illite-Fe-smectite problem: A critical review. *Terra Nova* **2007**, *19*, 95–104. [CrossRef]

31.　McRae, S.G. Glauconite. *Earth-Sci. Rev.* **1972**, *8*, 397–440. [CrossRef]

32.　Odin, G.S.; Matter, A. De glauconiarum origine. *Sedimentology* **1981**, *28*, 611–641. [CrossRef]

33.　Amorosi, A.; Sammartino, I.; Tateo, F. Evolution patterns of glaucony maturity: A mineralogical and geochemical approach. *Deep. Sea Res. Part II Top. Stud. Oceanogr.* **2007**, *54*, 1364–1374. [CrossRef]

34.　Amorosi, A. Glaucony and sequence stratigraphy: A conceptual framework of distribution in siliciclastic sequences. *J. Sediment. Res. B Stratigr. Glob. Stud.* **1995**, *B65*, 419–425.

35.　Baldermann, A.; Dietzel, M.; Mavromatis, V.; Mittermayr, F.; Warr, L.N.; Wemmer, K. The role of Fe on the formation and diagenesis of interstratified glauconite-smectite and illite-smectite: A case study of Upper Cretaceous shallow-water carbonates. *Chem. Geol.* **2017**, *453*, 21–34. [CrossRef]

36.　Banerjee, S.; Bansal, U.; Vilas Thorat, A. A review on palaeogeographic implications and temporal variation in glaucony composition. *J. Palaeogeogr.* **2016**, *5*, 43–71. [CrossRef]

37.　Banerjee, S.; Farouk, S.; Nagm, E.; Choudhury, T.R.; Meena, S.S. High Mg-glauconite in Campanian Duwi Formation of Abu Tartur Plateau, Egypt and its implications. *J. Afr. Earth Sci.* **2019**. [CrossRef]

38.　Rudmin, M.; Banerjee, S.; Mazurov, A. Compositional variation of glauconites in Upper Cretaceous-Paleogene sedimentary iron-ore deposits in South-eastern Western Siberia. *Sediment. Geol.* **2017**, *355*, 20–30. [CrossRef]

39.　Merchant, R.J. Glauconite-the future potash for fertilisers in New Zealand. *AusIMM Bull.* **2012**, *1*, 78–81.

40.　Prakash, S.; Verma, J.P. Global perspective of potash for fertilizer production. In *Potassium Solubilizing Microorganisms for Sustainable Agriculture*; Meena, V., Maurya, B., Eds.; Springer: New Delhi, India, 2016; pp. 327–331.

41.　Franzosi, C.; Castro, L.N.; Celeda, A.M. Technical evaluation of glauconies as alternative potassium fertilizer from the Salamanca Formation, Patagonia, Southwest Argentina. *Nat. Resour. Res.* **2014**, *23*, 311–320. [CrossRef]

42.　Castro, L.; Tourn, S. Direct application of phosphate rocks and glauconite as alternative sources of fertilizer in Argentina. *Explor. Min. Geol.* **2003**, *12*, 71–78. [CrossRef]

43.　Karimi, E.; Abdolzadeh, A.; Sadeghipour, H.R.; Aminei, A. The potential of glauconitic sandstone as a potassium fertilizer for olive plants. *Arch. Agron. Soil Sci.* **2012**, *58*, 983–993. [CrossRef]

44.　Rudmin, M.; Banerjee, S.; Mazurov, A.; Makarov, B.; Martemyanov, D. Economic potential of glauconitic rocks in Bakchar deposit (S-E Western Siberia) for alternate potash fertilizer. *Appl. Clay Sci.* **2017**, *150*, 225–233. [CrossRef]

45.　Rudmin, M.; Oskina, Y.; Banerjee, S.; Mazurov, A.; Soktoev, B.; Shaldybin, M. Roasting-leaching experiments on glauconitic rocks of Bakchar ironstone deposit (Western Siberia) for evaluation their fertilizer potential. *Appl. Clay Sci.* **2018**, *162*, 121–128. [CrossRef]

46.　Rudmin, M.; Banerjee, S.; Makarov, B.; Mazurov, A.; Ruban, A.; Oskina, Y.; Tolkachev, O.; Buyakov, A.; Shaldybin, M. An investigation of plant growth by the addition of glauconitic fertilizer. *Appl. Clay Sci.* **2019**, *180*, 105178. [CrossRef]

47.　Drits, V.A.; Ivanovskaya, T.A.; Sakharov, B.A.; Zvyagina, B.B.; Derkowski, A.; Gor'kova, N.V.; Pokrovskaya, E.V.; Savichev, A.T.; Zaitseva, T.S. Nature of the structural and crystal-chemical heterogeneity of the Mg-rich glauconite (Riphean, Anabar Uplift). *Lithol. Miner. Resour.* **2010**, *45*, 555–576. [CrossRef]

48. Zviagina, B.B.; Drits, V.A.; Sakharov, B.A.; Ivanovskaya, T.A.; Dorzhieva, O.V.; McCarty, D.K. Crystal-chemical regularities and identification criteria in fe-bearing k-dioctahedral micas 1 m from X-Ray diffraction and infrared spectroscopy data. *Clays Clay Miner.* **2017**, *65*, 234–251. [CrossRef]

49. Rashidzadeh, A.; Olad, A. Slow-released NPK fertilizer encapsulated by NaAlg-g-poly(AA-co-AAm)/MMT superabsorbent nanocomposite. *Carbohydr. Polym.* **2014**, *114*, 269–278. [CrossRef] [PubMed]

50. Chen, L.; Chen, X.L.; Zhou, C.H.; Yang, H.M.; Ji, S.F.; Tong, D.S.; Zhong, Z.K.; Yu, W.H.; Chu, M.Q. Environmental-friendly montmorillonite-biochar composites: Facile production and tunable adsorption-release of ammonium and phosphate. *J. Clean. Prod.* **2017**, *156*, 648–659. [CrossRef]

51. Liang, D.; Zhang, Q.; Zhang, W.; Liu, L.; Liang, H.; Quirino, R.L.; Chen, J.; Liu, M.; Lu, Q.; Zhang, C. Tunable thermo-physical performance of castor oil-based polyurethanes with tailored release of coated fertilizers. *J. Clean. Prod.* **2019**, *210*, 1207–1215. [CrossRef]